Clinical Cancer Research

SIRPα-Antibody Fusion Proteins Selectively Bind and Eliminate Dual Antigen-Expressing Tumor Cells

Emily C. Piccione, Silvia Juarez, Serena Tseng, Jie Liu, Melissa Stafford, Cyndhavi Narayanan, Lijuan Wang, Kipp Weiskopf, and Ravindra Majeti

Abstract

Purpose: CD47 is highly expressed on a variety of tumor cells. The interaction of CD47 with signal regulatory protein alpha (SIRPα), a protein on phagocytic cells, transmits a "don't eat me" signal that negatively regulates phagocytosis. CD47–SIRPα antagonists enable phagocytosis by disrupting the inhibitory signal and can synergize with Fc-mediated pro-phagocytic signals for potent elimination of tumor cells. A potential limitation of therapeutic CD47–SIRPα antagonists is that expression of CD47 on normal cells may create sites of toxicity or an "antigen sink." To overcome these limitations and address selective tumor targeting, we developed SIRPabodies to improve the therapeutic benefits of CD47–SIRPα blockade specifically toward tumor.

Experimental Design: SIRPabodies were generated by grafting the wild-type SIRPα either to the N-terminus or to the C-terminus of the heavy chain of rituximab. Selective tumor binding was tested using CFSE-labeled human primary CLL cells in the presence of 20-fold excess of human RBCs. NSG mice were transplanted with Raji-luciferase cells and were assigned to controls versus SIRPabody treatment. Cynomolgus nonhuman primates were administered a single intravenous infusion of SIRPabody at 3, 10, or 30 mg/kg.

Results: SIRPabodies selectively bound to dual antigen-expressing tumor cells in the presence of a large antigen sink. SIRPabody reduced tumor burden and extended survival in mouse xenograft lymphoma models. SIRPabody caused no significant toxicity in nonhuman primates.

Conclusions: These findings establish SIRPabodies as a promising approach to deliver the therapeutic benefit of CD47–SIRPα blockade specifically toward tumor cells. SIRPabodies may be applied to additional cancer types by grafting SIRPα onto other tumor-specific therapeutic antibodies. *Clin Cancer Res; 22(20); 5109–19. ©2016 AACR.*

Introduction

CD47 is a transmembrane protein, which is widely expressed on many cell types and serves as a ligand for signal regulatory protein alpha (SIRPα), a receptor on phagocytic cells including macrophages and dendritic cells (1). This interaction transmits a "don't eat me" signal by initiating signaling cascades that ultimately inhibit phagocytosis (2–5). Elevated CD47 expression relative to normal cell counterparts has been detected on acute myeloid leukemia stem cells (AML LSC), multiple subtypes of B-cell non-Hodgkin lymphoma (NHL), and many human solid tumor cells (6–9). CD47 contributes to cancer pathogenesis by enabling tumor cells to evade phagocytosis, and disruption of the CD47–SIRPα interaction is a therapeutic strategy to induce phagocytic elimination of tumor cells (10). However, wide distribution of CD47 on normal cells may represent potential sites of toxicity or an "antigen sink" that could prevent CD47-targeting agents from reaching tumor cells at therapeutically relevant doses.

The N-terminus of SIRPα contains an immunoglobulin superfamily V-like fold that interacts with the N-terminus of CD47 (11, 12). The CD47–SIRPα interaction can be antagonized with antibodies that bind to the interaction interface on either protein or with recombinant SIRPα (6, 13, 14). However, the native interaction between CD47 and SIRPα is relatively weak, and this may limit the utility of wild-type SIRPα as a therapeutic agent (13, 15). To address this issue, High-affinity variants of SIRPα were generated and shown to antagonize the interaction and induce phagocytosis in settings where a pro-phagocytic Fc domain was present (13).

Antibody Fc domains can serve as pro-phagocytic signals by binding to Fc receptors (FcR) on phagocytic effector cells and triggering antibody-dependent cellular phagocytosis (ADCP; ref. 16). CD47–SIRPα antagonists enable phagocytosis by blocking an inhibitory signal and have been shown to synergize with pro-phagocytic Fc-mediated signals. Synergy was initially shown with blocking anti-CD47 antibodies and rituximab, an anti-CD20 antibody known to activate FcRs (7). Synergistic cell elimination was also observed between trastuzumab and anti-CD47 or anti-SIRPα antibodies (17). High-affinity SIRPα monomers also enabled synergistic induction of phagocytosis when combined with tumor-specific monoclonal antibodies including trastuzumab, rituximab, and cetuximab (13). Taken together, these studies demonstrate the potential for CD47–SIRPα antagonists to synergize with tumor-specific monoclonal antibodies to induce potent elimination of tumor cells by phagocytosis.

Division of Hematology, Department of Medicine, Cancer Institute, and Institute for Stem Cell Biology and Regenerative Medicine, Stanford University, Stanford, California.

Note: Supplementary data for this article are available at Clinical Cancer Research Online (http://clincancerres.aacrjournals.org/).

Corresponding Author: Ravindra Majeti, Stanford University, 265 Campus Drive, G3021B, Palo Alto, CA 94305. Phone: 650-721-6376; Fax: 650-725-6910; E-mail: rmajeti@stanford.edu

doi: 10.1158/1078-0432.CCR-15-2503

Translational Relevance

Agents that block the CD47–SIRPα interaction synergize with pro-phagocytic FcR-activating antibodies, including the anti-CD20 antibody rituximab, for potent phagocytic elimination of tumor cells. We developed bispecific antibody variants targeting CD47 and CD20 to combine these two functions into a single molecule that recapitulated the potent synergistic effect of combination therapy with no toxic effects on normal cells. Our bispecific antibodies incorporate a blocking component with weak affinity for CD47, rendering them unable to bind normal cells expressing CD47 alone, and require simultaneous binding to CD20 for high avidity binding to dual antigen-expressing tumor cells. Such bispecific antibodies targeting CD47 along with tumor-associated antigens may be an effective strategy for selectively eliminating tumor cells that can be broadly applied to cancer.

We sought to develop a novel therapeutic antibody format that would disrupt the CD47–SIRPα interaction, deliver an Fc domain pro-phagocytic stimulus selectively to tumor cells, and lack toxicity against cells expressing CD47 alone. To achieve selective binding to tumor cells, our format uses a monoclonal antibody specific for an established tumor antigen as a scaffold. The N-terminal Ig domain of SIRPα was grafted onto the antibody scaffold to function as a CD47 antagonist. We hypothesized that the resulting "SIRPabodies" would deliver blockade of the CD47–SIRPα interaction specifically to cells expressing the tumor antigen as wild-type SIRPα interacts weakly with CD47, and that strong binding to tumor cells would depend on avidity contributions provided by binding to the tumor antigen. Moreover, by adding a CD47–SIRPα blocking component to an Fc-domain containing antibody, we predicted enhanced tumor elimination analogous to the synergy observed through combination of CD47–SIRPα blocking agents and FcR engagement. Here, we tested these hypotheses by generating SIRPabodies in a variety of formats using rituximab, an extensively studied anti-CD20 antibody, as the tumor-specific antibody for proof-of-concept studies. SIRPabodies were interrogated for binding specificity, therapeutic efficacy against human NHL *in vivo*, and toxicity in nonhuman primates.

Materials and Methods

SIRPabody construction, expression, and purification

The V_H and V_L from the 2B8 clone from which rituximab was generated were synthesized using custom gene synthesis (MCLAB) and subcloned into the pCEP4 mammalian expression vector (Invitrogen) containing the human C_{H1} or C_k genes, respectively, to create the heavy and light chains for expression of anti-CD20 (18). To create SIRPabodies, the N-terminal V-set Ig domain (residues 1-118) of the predominant allele of SIRPα (allele 2) was introduced onto the heavy chain of anti-CD20 via overlapping PCR with introduction of a linker (12, 19). The following linkers were used: CD20–2GL–SIRPα HC: $(GGGGS)_2$, CD20–4GL–SIRPα HC: $(GGGGS)_4$, SIRPα-γ-CD20 HC: ASTKGPSVFPLAP. Plasmids containing each chain were cotransfected into Freestyle 293 cells (Invitrogen) using 293 Fectin (Invitrogen) according to manufacturer's instructions. After 4 to 7 days, cell culture supernatant was prepared by spinning cell cultures at 300 × *g*. Supernatant containing antibody was subject to antibody purification by affinity chromatography on Protein A Sepharose (GE Healthcare Lifesciences). Purified antibody was dialyzed against PBS and analyzed by 10% SDS-PAGE (Invitrogen) under reducing and nonreducing conditions followed by Coomassie Brilliant Blue staining. Purified antibody was quantified by A280.

Antibodies

SIRPα-Fc (hIgG4) was described previously (13). Anti-CD47 (clone B6H12.2, mouse IgG1) was described previously (6). The V_L and V_H from B6H12.2 were subcloned into pCEP4 expression vector containing human C_k or C_{H1} genes, respectively, to create anti-CD47 (hIgG1). SIRPα-Fc and anti-CD47 were expressed and purified as described above. Human IgG1 isotype control antibody used for *in vitro* experiments was purchased from Sigma. Additional antibodies used for *in vivo* experiments are as follows: Rituximab (anti-CD20, human IgG1) was purchased from the Stanford University Medical Center, and mouse IgG from Innovate Research.

Cell lines

YB2/0, Raji, Daudi, ST486, and Ramos cell lines were purchased from ATCC. Raji cells expressing modified luciferase and eGFP were described previously (7). YB2/0 cells were engineered to stably express human CD20 cDNA (Genecopoeia) via an engineered transposable element (20). YB2/0 cells were engineered to stably express human CD47 by lentiviral transduction with virus generated from human CD47 cDNA (Open Biosystems, Thermo Scientific) in the pCDH backbone (System Biosciences).

Detection of antibody binding by flow cytometry

Cells were stained with primary antibodies at 10 μg/mL unless otherwise stated prior to staining with PE antihuman Fc secondary antibody (eBiosciences). Flow cytometry was performed using the BD FACSCanto II. For competition-based binding experiments, cells were stained with the indicated prior antibodies prior to staining with 10 μg/mL DyLight 488 anti-CD20 (2B8-hIgG1) or Alexa Fluor 647 anti-CD47 (clone B6H12.2; BD Biosciences). DyLight 488 anti-CD20 was generated by labeling purified antibody with the DyLight 488 Antibody Labeling Kit (Thermo Scientific) according to manufacturer's instructions.

Biacore

The kinetics of antibody binding to recombinant CD47 antigen were determined by surface plasmon resonance-based measurements with a Biacore 2000 instrument performed by Biosensor Tools. The test antibodies were diluted in 10 mmol/L sodium acetate pH 5.0 and amine coupled onto a GLM sensor chip. The CD47 antigen was a His-tagged monomer to allow for affinity measurements in the absence of avidity contributions. The antigen was injected over reaction matrices in a threefold dilution series. Each sample was injected across the antibody surface for 460 seconds. The association and dissociation rate constant, k_a ($M^{-1}s^{-1}$) and k_d (s^{-1}), respectively, were monitored, and a K_D value was determined.

Evaluation of simultaneous binding

Biotinylated human CD47-Fc fusion protein was incubated with DyLight 650-conjugated neutravidin (Pierce) to form CD47 tetramers. CD47 tetramers were coincubated with YB2/0 cells engineered to express human CD20 and the experimental antibodies. Antibody binding to cells was detected with a secondary PE antihuman Fc antibody (eBiosciences) and flow cytometry analysis. Gating on live cells and double positive (PE+DyLight 650+) events indicated simultaneous binding of primary antibody to CD47 and CD20.

Human samples

Human CLL samples were obtained from patients at the Stanford Medical Center with informed consent, according to an IRB-approved protocol (Stanford IRB # 6453). Human peripheral blood mononuclear cells (PBMC) and red blood cells (RBC) were from anonymous donors and were purchased from the Stanford Blood Center.

Cynomolgus macaque studies

Cynomolgus monkey whole blood used for *ex vivo* staining (Fig. 4B) was obtained from BioreclamationIVT. Toxicity studies in Cynomolgus macaques were performed by Charles River Laboratories (Reno, NV) in accordance with Association for Assessment and Accreditation of Laboratory Animal Care international guidelines. Male cynomolgus macaques weighing approximately 3 kg were administered a single dose of CD20–2GL–SIRPα HC by intravenous infusion. Flow cytometry analysis was performed by Flow Contract Site Laboratory (Kirkland, WA). Whole blood was stained with CD45 APC clone MB4606 (Miltenyi) and RBCs were discriminated as the $CD45^-$ population. Binding of CD20–2GL–SIRPα HC to RBCs was determined *ex vivo* by staining with PE antihuman Fc secondary (eBiosciences). Median fluorescence intensity values were derived from cytogram plots and converted to molecules of equivalent fluorochrome (MOEF) by collecting beads of known fluorescence, generating a standard curve and extrapolating the value using a spreadsheet supplied by the bead manufacturer (Spherotech). To assess depletion of B cells upon treatment with CD20–2GL–SIRPα HC, whole blood was treated with ACK lysis buffer (Life Technologies) and stained with CD45 APC (described above), CD3 FITC clone SP34 (BD Biosciences), and CD21 V450 clone B-ly4 (BD Biosciences). B cells were identified as $CD45^+$ $CD3^-$ $CD21^+$ cells.

In vivo antibody treatment

A total of 1×10^6 luciferase-labeled Raji cells were injected subcutaneously into the hind flank or intravenously into the tail vein of 6- to 10-week-old NOD. Cg-*Prkdcscid*Il2rgtm1Wjl/SzJ (NSG) mice. Mice were monitored for engraftment via bioluminescent imaging and daily intraperitoneal injections of 200 μg mouse IgG control, rituximab, SIRPα–hIgG4, CD20–2GL–SIRPα HC, or 200 μg SIRPα–hIgG4 + 200 μg rituximab were administered. Tumor progression was monitored with weekly bioluminescent imaging analysis and mice were followed for overall survival. All experiments were performed according to the Stanford University institutional animal guidelines.

Luciferase imaging analysis

Luciferase imaging analysis was performed as described previously (7).

Determination of serum levels of antibody by ELISA

Serum samples were collected from treated mice and antibody levels were determined by ELISA. ELISA plates were coated with goat antihuman antibody, Fcγ fragment specific (Jackson ImmunoResearch) and blocked with Superblock (Pierce) prior to incubation with serial dilutions of serum samples. Detection was carried out with antihuman kappa horseradish peroxidase antibody (Bethyl) as described above. Concentrations of antibody in

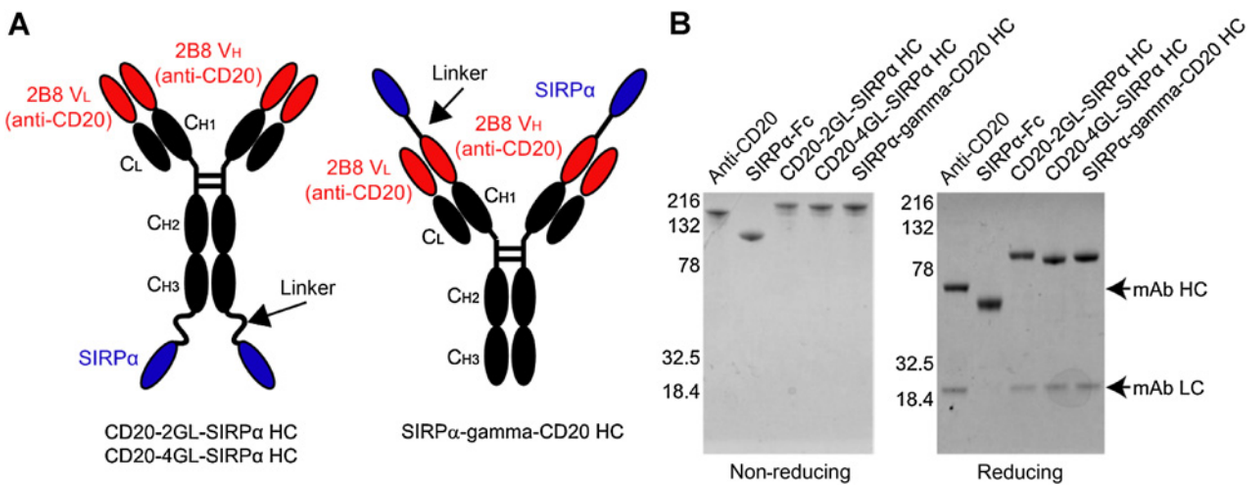

Figure 1.

SIRPabodies were produced as a single IgG-like species. **A,** schematic of SIRPabody molecules. The N-terminal Ig domain of wild-type SIRPα (blue) was grafted on the heavy chain of anti-CD20 (clone 2B8). Variable regions (V_H and V_L) of anti-CD20 are in red. Constant regions of anti-CD20 are human IgG1 isotype and are shown in black. Amino acid linkers are shown in black and sequences are listed in the Materials and Methods. **B,** SDS-PAGE of purified antibodies under nonreducing (left) and reducing (right) conditions. Sizes of heavy chain (HC) and light chain (LC) of unmodified monoclonal antibody are indicated.

serum samples were determined by extrapolation from standard curves using the four-parameter logistic fit.

Results

SIRPabodies bind strongly to CD20 and weakly to CD47

To create antibody-like molecules that block the CD47–SIRPα interaction and also require binding to a second tumor antigen for high avidity binding, we sought to exploit the low affinity of this interaction (11, 12, 15). CD20 was chosen as the target tumor antigen for initial proof-of-concept studies as rituximab, an anti-CD20 antibody, has been shown to synergize with CD47–SIRPα antagonists (7, 13). The N-terminal Ig domain of SIRPα was grafted onto either the N- or C-terminus of the heavy chain of rituximab (Fig. 1A). A 13 amino acid sequence derived from the N-terminal end of the CH1 domain was used for linkage to the N-terminus to create SIRPα-γ-CD20 HC. A flexible polyglycine-serine linker (GGGGS) of either two or four repeats was used to link SIRPα onto the C-terminus to make CD20–2GL–SIRPα HC or CD20–4GL–SIRPα HC, respectively. Each SIRPabody was produced as a single IgG-like species in mammalian cells and the increased size of the heavy chain relative to parental anti-CD20 is reflective of the addition of the SIRPα Ig domain (Fig. 1B).

SIRPabodies were evaluated for their ability to bind to antigen-expressing cells using rat cells engineered to express human CD20 or separately, human CD47. All SIRPabodies bound to CD20 in direct staining assays and blocked binding of labeled anti-CD20 in competition experiments with a similar potency as parental anti-CD20 (Fig. 2A and Supplementary Fig. S1A). The B6H12.2 anti-CD47 antibody has been extensively studied and served as a reference for robust CD47 binding (21). SIRPα-Fc and all SIRPabodies demonstrated weaker binding to CD47 than anti-CD47, which is indicative of the relatively low affinity of the CD47–SIRPα interaction (Fig. 2B). SIRPα-γ-CD20 HC, with SIRPα attached at the N-terminus, displayed comparable binding to CD47 as SIRPα-Fc control. In contrast, CD20–2GL–SIRPα HC and CD20–4GL–SIRPα HC each had reduced binding to CD47 relative to SIRPα-Fc, presumably due to steric hindrance of the CD47 binding site. All SIRPabodies were outcompeted by labeled anti-CD47 in competition experiments, consistent with their weaker interaction with CD47 (Supplementary Fig. S1B). Because weak binding to CD47 is a central component of our rationale, we quantitatively determined the affinity of each SIRPabody for monomeric CD47 using surface plasmon resonance analysis. All SIRPabodies had lower affinity for CD47 than B6H12.2, with SIRPα-γ-CD20 HC having an approximately 20-fold reduction

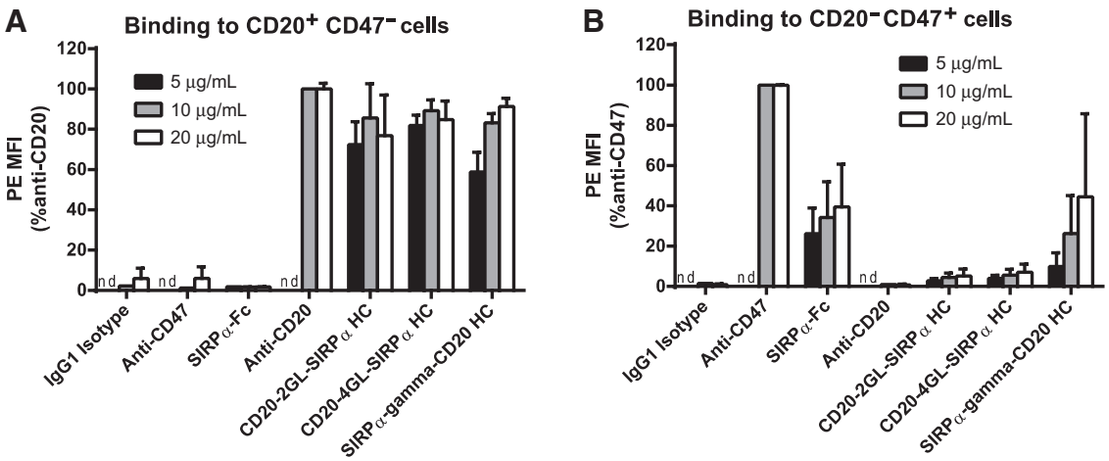

C

Antibody	K_D (nmol/L)
Anti-CD47	0.31
SIRPα-Fc	25.4
CD20-2GL-SIRPα HC	21.4
CD20-4GL-SIRPα HC	15.93
SIRPα-gamma-CD20 HC	6.39

Figure 2.

SIRPabodies bind strongly to CD20 and weakly to CD47. **A,** YB2/0 cells engineered to express human CD20 but not CD47 were stained with the indicated purified antibodies. Cells were subsequently stained with PE antihuman secondary and antibody staining was detected by flow cytometry. (mean ± SD, $n = 4$); nd, not determined. **B,** YB2/0 cells engineered to express human CD47 but not CD20 were stained with the indicated purified antibodies. Cells were subsequently stained with PE antihuman secondary and antibody staining was detected by flow cytometry. (mean ± SD, $n = 4$); nd, not determined. **C,** kinetic association and dissociation parameters, along with calculated affinity (Kd) for binding of the indicated antibodies to monomeric human CD47 antigen were measured by surface plasmon resonance using Biacore analysis.

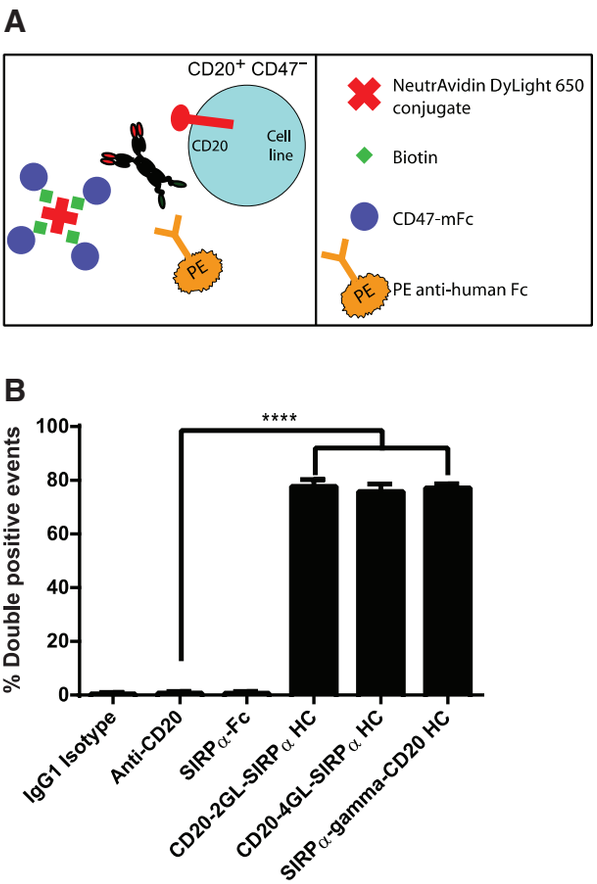

Figure 3.

SIRPabodies bind simultaneously to CD20 and CD47. **A,** schematic of experimental design to detect simultaneous binding to CD20 and CD47. Biotinylated CD47 antigen was linked to a fluorescent (DyLight 650) neutravidin tetramer which was co-incubated with unlabeled experimental antibody and $CD20^+CD47^-$YB2/0 cells. Experimental antibody binding was detected by staining with PE-conjugated antihuman secondary antibody. PE+DyLight 650+ live cells reflect simultaneous binding of experimental antibody to CD20 and CD47. **B,** PE+DyLight 650+ events were detected by flow cytometry and represent simultaneous binding to CD47 and CD20. ****, $P < 0.0001$, *t*-test, (mean ±SD, $n = 6$).

and CD20–2GL–SIRPα HC and CD20–4GL–SIRPα HC having more than 50-fold reduction (Fig. 2C). Collectively, these data show that the SIRPabodies retain strong binding to CD20 and that the strength of CD47 binding can be modulated based on the location of SIRPα attachment to the antibody molecule.

SIRPabodies bind simultaneously to CD47 and CD20

To address whether a single SIRPabody molecule could simultaneously bind to CD20 and CD47, cells expressing CD20 but not CD47 were incubated with SIRPabodies along with complexes containing a recombinant biotinylated CD47 antigen bound to neutravidin-fluorescent conjugates. Antibody binding to cells was then detected by flow cytometry with a secondary antibody conjugated to a different fluorophore, and double positive live cell events indicated simultaneous binding to each antigen (Fig. 3A). All SIRPabodies demonstrated simultaneous binding to each antigen (Fig. 3B). To address whether SIRPabodies bind to both CD20 and CD47 on dual antigen-expressing cells, Raji cells were incubated with SIRPabodies prior to staining with labeled anti-CD47 or labeled anti-CD20 (Supplementary Fig. S2). All SIRPabodies bound CD47 on Raji cells as indicated by blocking of labeled anti-CD47 antibody (Supplementary Fig. S2A). Importantly, the blocking of anti-CD47 observed with the SIRPabodies is due to enhanced avidity contributed by simultaneous binding to CD20, as SIRPα-Fc did not block as strongly due to its relatively weak affinity for CD47 (Supplementary Fig. S2A). The reciprocal experiment demonstrated binding of SIRPabodies to CD20 on Raji cells (Supplementary Fig. S2B). Collectively, these data demonstrate that CD20 and CD47 each contribute to SIRPabody binding to dual antigen-expressing cells.

SIRPabodies selectively bind to dual antigen–expressing tumor cells in the presence of a large antigen sink

A major rationale for generating SIRPabodies targeting CD47 along with a tumor-associated antigen is to avoid binding to cells that express CD47 alone while retaining the therapeutic benefit of blocking the CD47–SIRPα interaction on tumor cells. RBCs highly express CD47 and are a likely "antigen sink" as they are abundant and accessible to antibody in the bloodstream (22). To determine whether SIRPabodies selectively bind dual antigen-expressing cells in the presence of excess CD47-only expressing RBCs, CFSE-labeled tumor cells expressing CD47 and variable levels of CD20 were mixed with a 20-fold excess of unlabeled RBCs prior to incubation with antibody (Fig. 4A). Primary cells from three patients with B-cell chronic lymphocytic leukemia (B-CLL) were used as dual antigen-expressing cells in this assay as high expression of CD47 has been observed in this tumor type (Fig. 4B; ref. 7). All SIRPabodies, and the control anti-CD47 and anti-CD20, bound to tumor cells to a degree dependent on CD20 expression levels (Fig. 4C and Supplementary Fig. S3). In contrast, only anti-CD47 bound to RBCs, as indicated by a complete shift relative to isotype control. Importantly, all SIRPabodies did not bind to RBCs, indicating that weak binding to CD47 successfully eliminated binding to RBCs. Analysis of the distribution of cell types within the population of cells bound by each antibody revealed that, similar to anti-CD20, all SIRPabodies bound selectively to CLL cells in the presence of an antigen sink (Fig. 4D). Importantly, SIRPabody binding to tumor cells blocked subsequent staining with labeled anti-CD47, indicating that SIRPabody binding to tumor cells engages CD47 and is not solely driven by high-affinity binding to CD20 (Fig. 4E). Notably, the degree of blocking of labeled anti-CD47 corresponded to CD20 expression levels on tumor cells. Collectively, these data suggest that CD20 expression drives SIRPabody binding to tumor cells and that there is a threshold of CD20 expression that must be present on tumor cells to achieve CD47 blockade. This finding confirms that the SIRPabody approach directs CD47 blockade to dual antigen-expressing cells and successfully avoids targeting of cells expressing CD47 alone.

CD20–2GL–SIRPα HC reduces lymphoma burden and extends survival *in vivo*

CD20–2GL–SIRPα HC was chosen as a lead candidate for scaled up production and *in vivo* studies as the addition of SIRPα to the C-terminus resulted in weaker CD47 binding than addition to the N-terminus. Furthermore, we reasoned that the shorter

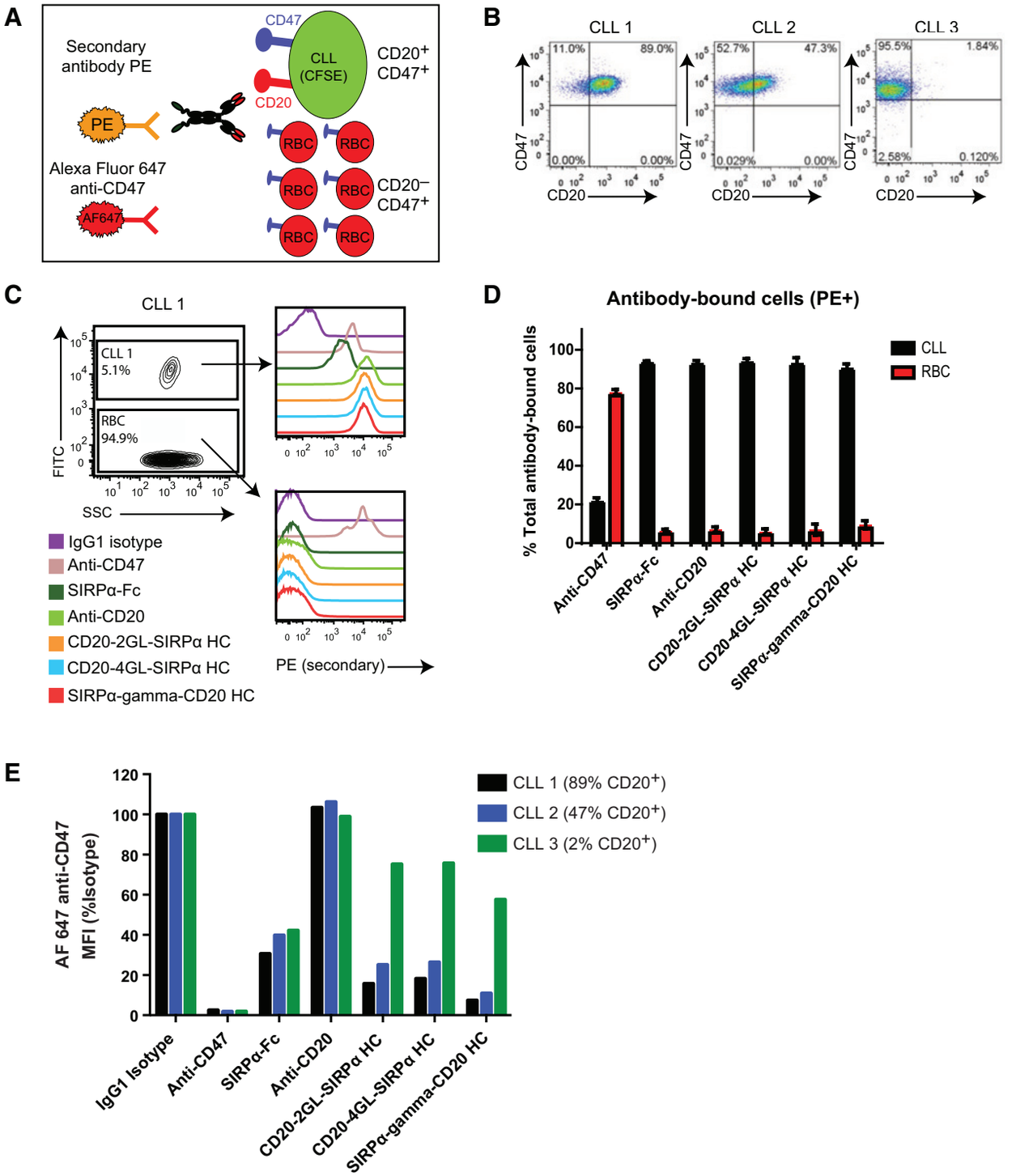

Figure 4.

SIRPabodies selectively bind to dual antigen-expressing cells in the presence of an antigen sink. **A,** experimental design to assay for selectivity in binding to dual antigen-expressing cells. CLL cells were labeled with CFSE and mixed with a 20-fold excess of CD20−CD47$^+$ human red blood cells (RBC). Cell mixtures were incubated with primary antibody prior to staining with PE anti-human Fc secondary and AF647 anti-CD47, and analysis by flow cytometry. **B,** CD47 and CD20 expression was profiled on three CLL samples by flow cytometry. **C,** CFSE$^+$ CLL cells were distinguished from CFSE$^-$ RBCs. Staining with 10 μg/mL primary antibody was detected with secondary antibody staining and flow cytometry. **D,** percentages of CLL cells (CFSE$^+$) and RBC (CFSE$^-$) within the antibody bound (PE+) population were determined. A single replicate from each donor was averaged together (mean ± SD, $n = 2$). **E,** binding of AF647 anti-CD47 to CLL cells is reported as MFI normalized to isotype control.

linker used in CD20–2GL–SIRPα HC would be less likely to be targeted for proteolytic cleavage *in vivo* compared to the longer linker of CD20–4GL–SIRPα HC. To test the *in vivo* therapeutic efficacy of CD20–2GL–SIRPα-HC, immunodeficient NSG mice were transplanted either subcutaneously or intravenously with luciferase-expressing Raji cells to model localized or disseminated lymphoma, respectively, as previously described (7, 23). Mice were treated with daily injections of control IgG, rituximab, SIRPα-Fc fusion protein, SIRPα-Fc plus rituximab, or CD20–2GL–SIRPα HC. In the subcutaneous model, SIRPα-Fc had no therapeutic effect relative to control IgG and did not augment rituximab activity when administered in combination (Fig. 5A). However, rituximab and CD20–2GL–SIRPα HC each reduced disease burden and extended survival relative to IgG control. CD20–2GL–SIRPα HC induced a statistically significant reduction in the median tumor volume compared to rituximab or rituximab plus SIRPα-Fc as measured by bioluminescence signal, which was further reflected in an increase in overall survival (Fig. 5B). In the disseminated lymphoma model, luciferase-labeled Raji cells were intravenously injected into NSG mice and followed for disease by bioluminescent imaging and for overall survival. Treatment with CD20–2GL–SIRPα HC significantly reduced tumor burden and extended survival relative to treatment with SIRPα-Fc, rituximab, or rituximab plus SIRPα-Fc (Fig. 5C and D). These data demonstrate that the CD20–2GL–SIRPα HC SIRPabody exhibits significantly improved *in vivo* efficacy compared to parental rituximab alone. Importantly, CD20–2GL–SIRPα HC and rituximab had similar pharmacokinetic profiles allowing direct comparison of therapeutic efficacy *in vivo*, and suggests that CD20–2GL–SIRPα HC is a viable therapeutic molecule for further development (Supplementary Fig. S4).

SIRPabodies effectively deplete target cells in nonhuman primates with no observed toxicity

To rigorously test the potential for CD20–2GL–SIRPα HC to bind to CD47 on RBCs, a titration of antibody was tested to see if significant binding to RBCs occurred at high concentrations (Fig. 6A and B). No binding to RBCs from humans or cynomolgus macaques was detected up to 500 μg/mL, in contrast to anti-CD47 control which demonstrated strong binding as low as 0.5 μg/mL. To address the potential for toxicity and binding to an antigen sink *in vivo*, cynomolgus macaques, which express a CD47 ortholog that is identical to human CD47 at the SIRPα interaction interface, were administered a single dose of CD20–2GL–SIRPα HC at 3, 10, or 30 mg/kg and followed for 2 weeks. Transient binding of CD20–2GL–SIRPα HC to RBCs was observed with the two highest doses, but binding did not lead to RBC depletion or substantial reduction in hemoglobin levels (Fig. 6C and E). As a pharmacodynamics marker, the percentage of B cells within the leukocyte compartment was determined by flow cytometry. Depletion of B cells was observed with all doses, indicating successful antibody delivery and cell targeting *in vivo* (Fig. 6D). Together, these data show that CD20–2GL–SIRPα HC effectively overcomes a physiologic antigen sink and depletes target cells *in vivo* with no observed RBC toxicity.

Discussion

We report here the generation of SIRPabodies, antibody-derivative candidate therapeutic molecules with wild-type SIRPα grafted onto an established tumor-targeting monoclonal antibody. The rationale for SIRPabodies is twofold: (i) to create a therapeutic molecule that delivers CD47–SIRPα blockade specifically to tumor cells and (ii) to recapitulate the synergistic effects of combining CD47–SIRPα blockade with a pro-phagocytic signal in the form of an Fc domain. Using the anti-CD20 antibody rituximab in proof-of-concept studies, we show that SIRPabodies achieve both of these goals, establishing them as promising novel cancer-targeting agents.

Disruption of the CD47–SIRPα interaction has been explored as a therapeutic strategy through several approaches including monoclonal antibody targeting of CD47 or SIRPα and recombinant SIRPα proteins that antagonize the interaction (6, 13, 14, 17). However, although these strategies exploit the elevated CD47 expression observed on tumor cells, they do not address the need for tumor cell selectivity. CD47 is widely expressed at low levels on most normal cell types, including RBCs and leukocytes. Normal cells expressing CD47 create an "antigen sink" that may sequester CD47 targeting agents, preventing these agents from binding to tumor cells *in vivo*. Moreover, undesired binding of CD47 targeting agents to normal cells may lead to toxicity, particularly anemia due to RBC phagocytic elimination. To overcome these limitations and direct the benefit of CD47–SIRPα blockade specifically to tumor cells, we created SIRPabodies with wild-type SIRPα engineered onto an established tumor-specific monoclonal antibody. We hypothesized that the low affinity of wild-type SIRPα for CD47 would facilitate weak binding of SIRPabodies to cells expressing CD47 alone. In contrast, on dual antigen-expressing tumor cells, SIRPabodies would bind strongly to the tumor-associated antigen and utilize CD47 binding as an additional source of interactions leading to avid binding. Consistent with this hypothesis, SIRPabodies bound weakly to cells expressing CD47 without CD20 (Fig. 2B and Supplementary Figs. S1B, S4A, and S4B) and bound to both antigens on dual antigen-expressing cells (Fig. 3B and Supplementary Fig. S2). These properties enabled SIRPabodies to selectively bind to tumor cells in the context of competition with 20-fold excess of RBCs expressing CD47 alone (Fig. 4). RBCs represent a large antigen sink and potential source of toxicity with CD47 targeting agents as CD47 expression regulates RBC clearance *in vivo* (22, 24). Surprisingly, SIRPabodies and wild-type SIRPα did not exhibit any detectable binding to RBC, even at high concentrations (Figs. 4C, 4D, 6A, and 6B). This may be due to a lack of crosslinking of CD47 by SIRPα on the surface of RBCs, as preincubation of RBCs with antibody that crosslinks CD47 has been shown to increase subsequent SIRPα binding to RBCs (25). Importantly, CD20–2GL–SIRPα HC did not cause anemia, or other toxicity, in nonhuman primates. As previously reported, we have developed a novel anti-CD47 humanized monoclonal antibody, Hu5F9-G4 (26). With single-dose administration of Hu5F9-G4 at 0, 0.1, 0.3, 1, 3, 10, and 30 mg/kg in nonhuman primates, Hu5F9-G4 caused a transient and dose-dependent anemia. Administration of 1, 3, or 10 mg/kg of Hu5F9-G4 in NHPs resulted in a nadir of hemoglobin level below 10 g/dL between days 5 and 7. One of the NHPs administered 30 mg/kg of Hu5F9-G4 developed severe anemia with a hemoglobin level that dropped below 8 g/dL. In contrast, none of NHPs that received CD20–2GL–SIRPα HC up to 30 mg/kg developed a hemoglobin level below 10 g/dL, indicating that the SIRPabody strategy successfully avoids toxicity and functional binding to a potential antigen sink created by circulating RBCs (Fig. 6).

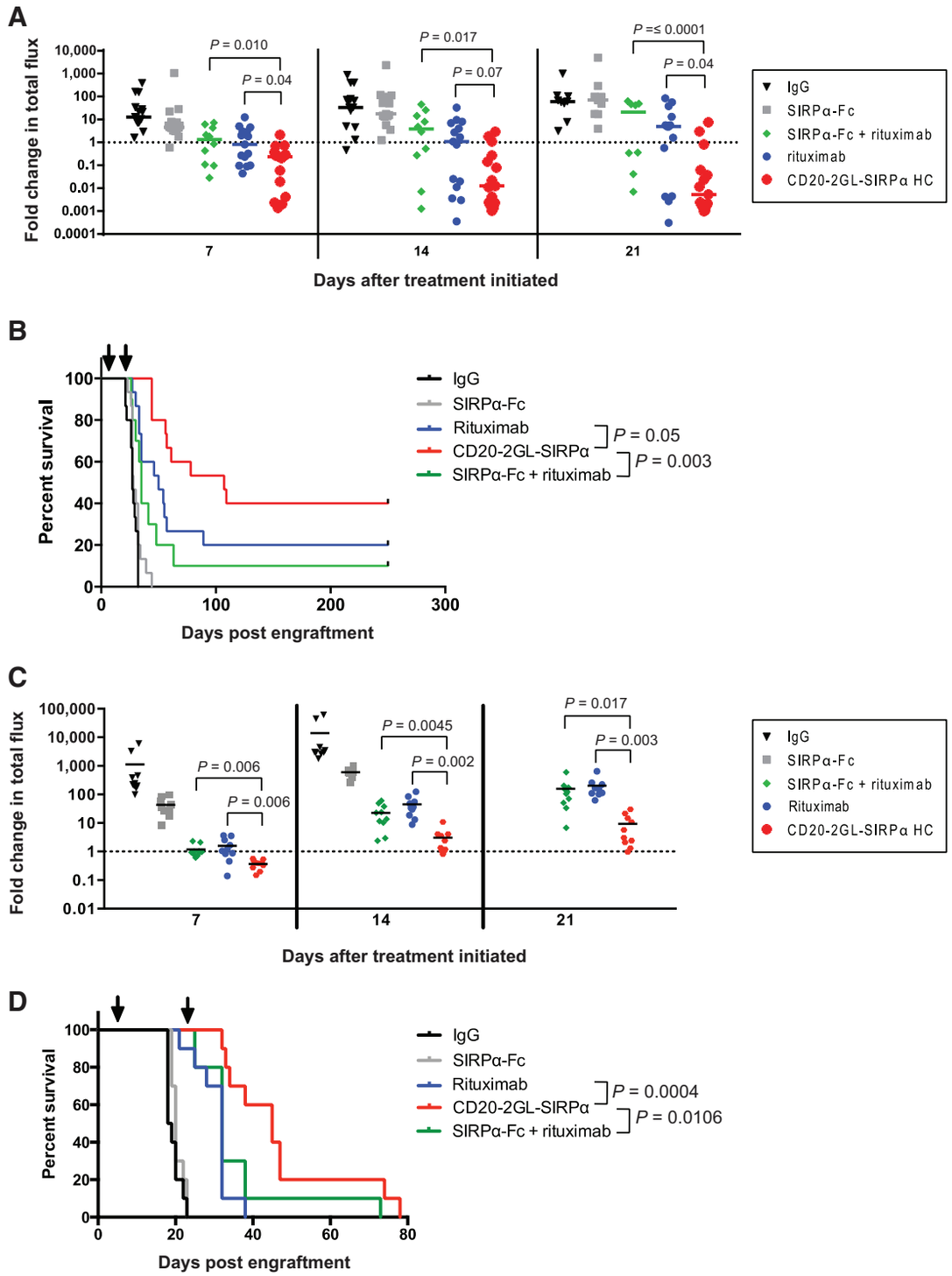

Figure 5.

CD20-2GL-SIRPα HC reduces lymphoma burden and extends survival *in vivo*. **A,** NSG mice were transplanted subcutaneously with Raji-luciferase cells. Seven days later, mice were treated with 14 daily doses of 200 μg IgG ($n = 15$), SIRPα-Fc ($n = 15$), rituximab ($n = 15$), CD20-2GL-SIRPα HC ($n = 15$), or 200 μg SIRPα-Fc + 200 μg rituximab ($n = 10$). Expansion of Raji-luciferase cells was evaluated by bioluminescence imaging. Each point represents a measurement from an independent mouse and lines indicate median values for each treatment group. *P* values were derived by *t*-test. **B,** Kaplan–Meier survival analysis was performed. Arrows indicated start (day 7) and stop (day 21) of treatment. Statistical analysis was performed by Mantel–Cox. **C,** NSG mice were transplanted intravenously with Raji-luciferase cells. Four days later, mice were administered 21 daily doses of antibody treatment as described in **A.** Each point represents a measurement from an independent mouse ($n = 10$). Lines indicate mean values for each treatment group. *P* values were derived by *t*-test. **D,** Kaplan–Meier survival analysis was performed. Arrows indicated start (day 4) and stop (day 25) of treatment. Statistical analysis was performed by Mantel–Cox.

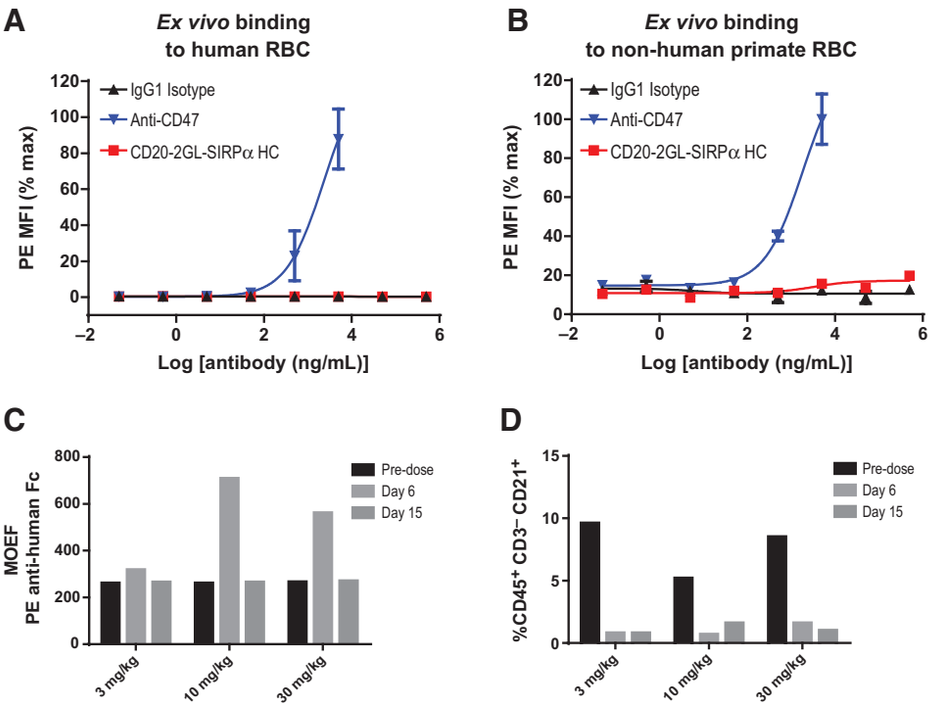

Figure 6.
SIRPabodies effectively deplete target cells in non-human primates with no observed toxicity. **A,** human RBCs were stained with the indicated antibodies over a range of concentrations prior to staining with PE antihuman secondary and detection by flow cytometry. MFI of the PE signal was determined and all data were normalized to the maximum signal observed. **B,** RBCs from cynomolgus macaques were stained and analyzed as in **A. C,** cynomolgus nonhuman primates were administered a single intravenous infusion of CD20-2GL-SIRPα HC at 3, 10, or 30 mg/kg. Blood samples were collected from each animal at the indicated time points. Binding of CD20-2GL-SIRPα HC to RBCs *in vivo* was detected by *ex vivo* staining with PE anti-human Fc secondary antibody. PE signal was detected by flow cytometry and molecules of equivalent fluorochrome (MEF) values were derived by extrapolation from a standard curve. **D,** blood samples were collected from each animal at the indicated time points. The percentage of B cells ($CD3^-$ $CD21^+$) within the leukocyte fraction ($CD45^+$) was determined by flow cytometry. **E,** hematologic values of cynomolgus macaques treated with CD20-2GL-SIRPα HC.

E

		RBC	Hgb	Retic	WBC	Plt
Treatment	**Day**	10^6/μL	g/dL	10^9/L	10^3/μL	10^3/μL
CD20-2GL-SIRPα HC 3 mg/kg	Prestudy	6.48	15.1	96.8	11.44	481
	3	5.73	13.2	69.0	6.46	365
	6	5.73	13.2	104.0	9.26	445
	8	5.55	12.8	192.9	10.94	548
	15	5.92	13.8	253.1	10.06	575
CD20-2GL-SIRPα HC 10 mg/kg	Prestudy	5.85	13.6	77.5	11.11	361
	3	5.25	12.2	87.2	14.40	239
	6	5.12	11.7	126.2	13.07	296
	8	5.10	11.7	206.9	11.27	386
	15	5.63	12.8	279.2	14.29	444
CD20-2GL-SIRPα HC 30 mg/kg	Prestudy	6.45	14.4	74.0	7.51	482
	3	5.38	12.0	59.5	6.92	279
	6	5.38	11.5	148.6	5.91	479
	8	5.24	11.2	268.5	6.03	504
	15	6.08	12.8	268.8	7.56	752

There is mounting evidence that therapeutic agents that block the CD47–SIRPα interaction may require an Fc component to achieve maximum therapeutic potency. Antibodies directed against CD47 have been shown to synergize with rituximab or trastuzumab, which are known to engage FcR (7, 17). As a proof-of-principle study, we developed bispecific antibodies (BsAbs) that cotarget CD47 and CD20 with reduced affinity for CD47 relative to the parental antibody, but retaining strong binding to CD20 (27). These characteristics facilitated selective binding of BsAbs to tumor cells, leading to phagocytosis. Treatment of human NHL-engrafted mice with BsAbs reduced lymphoma burden and extended survival while recapitulating the synergistic efficacy of anti-CD47 and anti-CD20 combination therapy. High-affinity SIRPα monomers developed as antagonists of the CD47–SIRPα interaction induced phagocytosis when presented as Fc fusion proteins, but failed to induce phagocytosis in monomeric form or when presented as a dimer lacking the Fc domain. This property allowed SIRPα monomers to function as adjuvants to increase the efficacy of Fc-containing tumor-specific antibodies including trastuzumab, rituximab, and cetuximab (13). Collectively, studies with high-affinity SIRPα monomers demonstrated a requirement for a pro-phagocytic FcR-activating signal in conjunction with CD47–SIRPα antagonism. We sought to introduce the benefits of CD47–SIRPα antagonism and FcR interaction into a single SIRPabody molecule. This strategy differs from monoclonal antibodies directed against CD47 or SIRPα and SIRPα-Fc fusion proteins as the SIRPabody presents the opportunity for selective binding to tumor cells through the introduction of additional tumor-specific binding regions. We hypothesized that SIRPabodies would be more potent than rituximab or SIRPα-Fc alone, as CD47–SIRPα blockade and FcR binding present two strategies for phagocytic induction, and incorporation into a single molecule should provide avidity contributions to overcome the low affinity of wild-type SIRPα for CD47.

CD20–2GL–SIRPα HC demonstrated a significant increase in efficacy relative to rituximab *in vivo*, particularly in the more aggressive disseminated lymphoma model (Fig. 5). The observed therapeutic effect is most likely due to phagocytosis, as experiments were performed in NSG mice, which lack functional B, T, and NK cells and are therefore devoid of other effector mechanisms (7, 23).

All SIRPabodies were able to bind CD20 and achieve the desired selectivity for dual antigen-expressing tumor cells. Importantly, this selectivity permitted potent depletion of target cells with no observed toxicity in nonhuman primates, which possess a large antigen sink. Moreover, SIRPabodies, which incorporate multiple pro-phagocytic functions into a single molecule, are more efficacious than monospecific agents that utilize a single pro-phagocytic mechanism for tumor reduction. Thus, SIRPabodies demonstrate highly selective binding properties, potent therapeutic efficacy *in vivo*, and lack of toxicity in nonhuman primates, establishing this approach as a promising strategy to direct the therapeutic benefit of CD47–SIRPα blockade directly to tumor cells.

Disclosure of Potential Conflicts of Interest

K. Weiskopf holds ownership interest in Alexo Therapeutics, Forty Seven Inc., and Stanford University for patent applications; and is a consultant/advisory board member for Alexo Therapeutics and Forty Seven Inc. R. Majeti holds ownership interest (including patents) in and is a consultant/advisory board member for Forty Seven Inc. No potential conflicts of interest were disclosed by the other authors.

Disclaimer

R. Majeti is a co-inventor of U.S. Patent No. 8,562,997 entitled "Methods of Treating Acute Myeloid Leukemia by Blocking CD47" and U.S. Patent No. 8,758,750 entitled "Synergistic Anti-CD47 Therapy for Hematologic Cancers." R. Majeti and E.C. Piccione are co-inventors of a U.S. patent application entitled "SIRP-Alpha Antibody Fusion Proteins."

Authors' Contributions

Conception and design: E.C. Piccione, L. Wang, K. Weiskopf, R. Majeti
Development of methodology: E.C. Piccione, J. Liu, L. Wang, K. Weiskopf, R. Majeti
Acquisition of data (provided animals, acquired and managed patients, provided facilities, etc.): E.C. Piccione, S. Juarez, S. Tseng, M. Stafford, C. Narayanan, R. Majeti
Analysis and interpretation of data (e.g., statistical analysis, biostatistics, computational analysis): E.C. Piccione, S. Juarez, J. Liu, L. Wang, R. Majeti
Writing, review, and/or revision of the manuscript: E.C. Piccione, J. Liu, K. Weiskopf, R. Majeti
Administrative, technical, or material support (i.e., reporting or organizing data, constructing databases): R. Majeti
Study supervision: J. Liu, R. Majeti

Acknowledgments

The authors thank Adriel Cha, Stephen Willingham, Aaron Ring, and Ryan Corces-Zimmerman for reagents, Feifei Zhao for laboratory management, and Irv Weissman for discussion.

Grant Support

This research was supported by a Translational Research Program Award from the Leukemia and Lymphoma Society (R. Majeti), the New York Stem Cell Foundation, funding from the J. Benjamin Eckenhoff Memorial Foundation, and funding from the Virginia and D. K. Ludwig Fund for Cancer Research. E.C. Piccione is supported by an NIH T32 Ruth L. Kirschstein National Research Service Award (AI07290). R. Majeti holds a Career Award for Medical Scientists from the Burroughs Wellcome Fund and is a New York Stem Cell Foundation - Robertson Investigator.

The costs of publication of this article were defrayed in part by the payment of page charges. This article must therefore be hereby marked *advertisement* in accordance with 18 U.S.C. Section 1734 solely to indicate this fact.

Received October 14, 2015; revised March 30, 2016; accepted April 5, 2016; published OnlineFirst April 28, 2016.

References

1. Brown EJ, Frazier WA. Integrin-associated protein (CD47) and its ligands. Trends Cell Biol 2001;11:130–5.
2. Jiang P, Lagenaur CF, Narayanan V. Integrin-associated protein is a ligand for the P84 neural adhesion molecule. J Biol Chem 1999;274:559–62.
3. Seiffert M, Brossart P, Cant C, Cella M, Colonna M, Brugger W, et al. Signal-regulatory protein alpha (SIRPalpha) but not SIRPbeta is involved in T-cell activation, binds to CD47 with high affinity, and is expressed on immature CD34(+)CD38(-) hematopoietic cells. Blood 2001;97:2741–9.
4. Barclay AN, Brown MH. The SIRP family of receptors and immune regulation. Nat Rev Immunol 2006;6:457–64.
5. Tsai RK, Discher DE. Inhibition of "self" engulfment through deactivation of myosin-II at the phagocytic synapse between human cells. J Cell Biol 2008;180:989–1003.
6. Majeti R, Chao MP, Alizadeh AA, Pang WW, Jaiswal S, Gibbs KD Jr, et al. CD47 is an adverse prognostic factor and therapeutic antibody target on human acute myeloid leukemia stem cells. Cell 2009;138:286–99.
7. Chao MP, Alizadeh AA, Tang C, Myklebust JH, Varghese B, Gill S, et al. Anti-CD47 antibody synergizes with rituximab to promote phagocytosis and eradicate non-Hodgkin lymphoma. Cell 2010;142:699–713.
8. Willingham SB, Volkmer JP, Gentles AJ, Sahoo D, Dalerba P, Mitra SS, et al. The CD47-signal regulatory protein alpha (SIRPa) interaction is a therapeutic target for human solid tumors. Proc Natl Acad Sci U S A 2012;109:6662–7.
9. Chao MP, Alizadeh AA, Tang C, Jan M, Weissman-Tsukamoto R, Zhao F, et al. Therapeutic antibody targeting of CD47 eliminates human acute lymphoblastic leukemia. Cancer Res 2011;71:1374–84.
10. Jaiswal S, Jamieson CH, Pang WW, Park CY, Chao MP, Majeti R, et al. CD47 is upregulated on circulating hematopoietic stem cells and leukemia cells to avoid phagocytosis. Cell 2009;138:271–85.
11. Hatherley D, Graham SC, Turner J, Harlos K, Stuart DI, Barclay AN. Paired receptor specificity explained by structures of signal regulatory proteins alone and complexed with CD47. Mol Cell 2008;31:266–77.
12. Hatherley D, Harlos K, Dunlop DC, Stuart DI, Barclay AN. The structure of the macrophage signal regulatory protein alpha (SIRPalpha) inhibitory receptor reveals a binding face reminiscent of that used by T cell receptors. J Biol Chem 2007;282:14567–75.
13. Weiskopf K, Ring AM, Ho CC, Volkmer JP, Levin AM, Volkmer AK, et al. Engineered SIRPalpha variants as immunotherapeutic adjuvants to anticancer antibodies. Science 2013;341:88–91.
14. Theocharides AP, Jin L, Cheng PY, Prasolava TK, Malko AV, Ho JM, et al. Disruption of SIRPalpha signaling in macrophages eliminates human acute myeloid leukemia stem cells in xenografts. J Exp Med 2012;209:1883–99.
15. Brooke G, Holbrook JD, Brown MH, Barclay AN. Human lymphocytes interact directly with CD47 through a novel member of the signal regulatory protein (SIRP) family. J Immunol 2004;173:2562–70.
16. Weiner LM, Surana R, Wang S. Monoclonal antibodies: versatile platforms for cancer immunotherapy. Nat Rev Immunol 2010;10:317–27.
17. Zhao XW, van Beek EM, Schornagel K, Van der Maaden H, Van Houdt M, Otten MA, et al. CD47-signal regulatory protein-alpha (SIRPalpha) interactions form a barrier for antibody-mediated tumor cell destruction. Proc Natl Acad Sci U S A 2011;108:18342–7.
18. Reff ME, Carner K, Chambers KS, Chinn PC, Leonard JE, Raab R, et al. Depletion of B cells *in vivo* by a chimeric mouse human monoclonal antibody to CD20. Blood 1994;83:435–45.
19. Takenaka K, Prasolava TK, Wang JC, Mortin-Toth SM, Khalouei S, Gan OI, et al. Polymorphism in Sirpa modulates engraftment of human hematopoietic stem cells. Nat Immunol 2007;8:1313–23.

20. Huang X, Wilber AC, Bao L, Tuong D, Tolar J, Orchard PJ, et al. Stable gene transfer and expression in human primary T cells by the Sleeping Beauty transposon system. Blood 2006;107:483–91.
21. Gresham HD, Goodwin JL, Allen PM, Anderson DC, Brown EJ. A novel member of the integrin receptor family mediates Arg-Gly-Asp-stimulated neutrophil phagocytosis. J Cell Biol 1989;108:1935–43.
22. Khandelwal S, van Rooijen N, Saxena RK. Reduced expression of CD47 during murine red blood cell (RBC) senescence and its role in RBC clearance from the circulation. Transfusion 2007;47:1725–32.
23. Shultz LD, Lyons BL, Burzenski LM, Gott B, Chen X, Chaleff S, et al. Human lymphoid and myeloid cell development in NOD/LtSz-scid IL2R gamma null mice engrafted with mobilized human hemopoietic stem cells. J Immunol 2005;174:6477–89.
24. Oldenborg PA, Zheleznyak A, Fang YF, Lagenaur CF, Gresham HD, Lindberg FP. Role of CD47 as a marker of self on red blood cells. Science 2000;288:2051–4.
25. Subramanian S, Parthasarathy R, Sen S, Boder ET, Discher DE. Species- and cell type-specific interactions between CD47 and human SIRPalpha. Blood 2006;107:2548–56.
26. Liu J, Wang L, Zhao F, Tseng S, Narayanan C, Shura L, et al. Pre-clinical development of a humanized anti-CD47 antibody with anti-cancer therapeutic potential. PloS ONE 2015;10:e0137345.
27. Piccione EC, Juarez S, Liu J, Tseng S, Ryan CE, Narayanan C, et al. A bispecific antibody targeting CD47 and CD20 selectively binds and eliminates dual antigen expressing lymphoma cells. mAbs 2015;7:946–56.